4:th CEAS Air & Space Conference
FTF Congress: Flygteknik 2013

Modeling of backlash in drivetrains

C. L. Akoto, H. Spangenberg
German Aerospace Center e.V.

Keywords: *drivetrain, backlash, inertia, elasticity, damping*

Abstract

The presence of backlash in drivetrains is a major source of limitations as it introduces nonlinearities that reduce their efficiency in speed and position control. Existing models in backlash assume massless shaft, and use only elasticity and damping properties to describe the transmitted torque. This assumption makes them inaccurate since it does not account for the contribution of the body's inertia. Thus, a new and simple model that takes into account the rotational inertia, elasticity and damping properties is proposed. The importance and validity of this approach is shown analytically, graphically and with an example of a simple failure case of shaft rupture. Preliminary analysis shows that real system behavior is predicted more closely than in previous model. Thus, the new model can be used for better prediction of system behavior for definition and optimization.

Abbreviations and terms

θ :	Angular displacement
α :	Half of backlash angle
k :	Elasticity
c :	Internal damping
j :	Inertia
T :	Torque
SDOF:	Single Degree of Freedom
PPM:	Phase plane model
JCK:	Inertia Damping Elasticity

Backlash: Clearance between mating gear teeth

1 Introduction

The presence of backlash in drivetrains is a major source of limitations that introduces nonlinearities in system behavior, a consequence of which might be problems with safety and/or reliability, which are crucial in the design of aerospace systems. This paper focuses on the analysis of existing backlash models followed by the proposal of a new modeling approach. In this study, some commonly used backlash models are examined. As an example a shaft model with backlash is considered. Many alternatives for estimating the effect of backlash in drivetrains exist. Some of these include the dead-zone model and the modified dead-zone model [1, 2]. On the other hand, there are limitations of the accuracy level of these models. Since existing backlash models differ in their results and do not predict system behavior

perfectly, a critical examination of the modeling approaches must be carried out to find an optimal approach for highly complex drivetrains.

For clarity, the highly complex drivetrain is replaced by a shaft with backlash which greatly reduces the complexity. Thus, a shaft with backlash is considered which is usually modeled as a massless shaft [1, 2]. This is a strong simplification since every shaft has a mass which is a measure of its inertia or its tendency to resist a motion induced by an external force. In [3] it is equally shown that the mass of a system is crucial in the study of noise and vibrations. An example where this importance is reflected is the undamped natural frequency of a translational system approximated as an SDOF. Given the mass (m) and the spring elasticity (k) the undamped natural frequency of the system is given by $\sqrt{k/m}$. This is an important aspect in system condition monitoring which is not reflected in the massless approximation of the shaft.

2 Modeling approaches

Previously used approaches in modeling of backlash are shown in Equations (1) to (4) [1, 2, 4, 5, 6 and 7].
Equation (1): is the dead zone approach [1, 2]. The approach approximates the shaft as a pure spring with no damping.
Equation (2): A commonly used modification of (1) known as the modified dead zone model [1, 2, 4], where damping has been introduced in the transmitted torque while maintaining the intervals.
Equation (3): This expression is obtained from the analysis of a massless beam [1, 2]. It keeps the same expression of the transmitted torque in (2), but introduces the elasticity and damping influences in the intervals
Equation (4): Represents the phase plane model, which was developed using the physical system represented by Equation (3). Its main difference from (3) is its new interval resulting from the phase plane analysis [1, 2].
Equation (5): Represents the physical system of the new modeling approach, enhancing (3) with inertia.
The simple approach described by Equation (1) will not be considered in the following analysis. Henceforth analysis will be mostly done on the modeling approaches of Equations (2) to (5).
An example of a shaft with backlash considered in this analysis is shown in Fig 1.

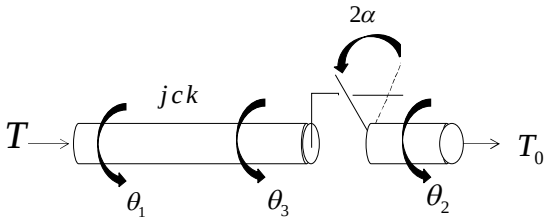

Fig. 1 Physical system: a shaft with backlash

The formulation of the new approach, supplements the approaches according to [1, 2] with the consideration of the inertia (j), elasticity (k), and inner damping (c) of the shaft. It is modeled such that the system is driven by a torque (T) on one end and outputs a torque (T_0) on the other end. The driving torque is expressed as a function of *displacement*, defined as $\theta_d(t)=\theta_1(t)-\theta_2(t)$, its time derivative $\dot{\theta}_d(t)=\dot{\theta}_1(t)-\dot{\theta}_2(t)$, and its second derivative $\ddot{\theta}_d(t)=\ddot{\theta}_1(t)-\ddot{\theta}_2(t)$ without using the state $\theta_3(t)$ [3]. The backlash angle is defined symmetrically as $\theta_3(t)-\theta_2(t)$ within the backlash gap 2α such that $|\theta_3(t)-\theta_2(t)|\le\alpha$.

$$T=\begin{cases} k(\theta_d-\alpha) & \theta_d>\alpha \\ 0 & |\theta_d|\le\alpha \\ k(\theta_d+\alpha) & \theta_d<-\alpha \end{cases} \quad (1)$$

$$T=\begin{cases} k(\theta_d-\alpha)+c\dot{\theta}_d & \theta_d>\alpha \\ 0 & |\theta_d|<\alpha \\ k(\theta_d+\alpha)+c\dot{\theta}_d & \theta_d<-\alpha \end{cases} \quad (2)$$

$$T=\begin{cases} 0 \;\; or \;\; k(\theta_d-\alpha)+c\dot{\theta}_d & \theta_d+(c/k)\dot{\theta}_d>\alpha \\ 0 & |\theta_d+(c/k)\dot{\theta}_d|\le\alpha \\ 0 \;\; or \;\; k(\theta_d+\alpha)+c\dot{\theta}_d & \theta_d+(c/k)\dot{\theta}_d<-\alpha \end{cases} \quad (3)$$

$$T = \begin{cases} k(\theta_d - \alpha) + c\dot{\theta}_d & (\theta_d, \dot{\theta}_d) \in A^+ \\ 0 & (\theta_d, \dot{\theta}_d) \in A^0 \\ k(\theta_d + \alpha) + c\dot{\theta}_d & (\theta_d, \dot{\theta}_d) \in A^- \end{cases} \quad (4)$$

Where:

$$A^+ = \left\{ (\theta_d, \dot{\theta}_d) : \begin{cases} f(\theta_d + \alpha, \dot{\theta}_d) \geq 2\alpha, & \dot{\theta}_d > 0 \\ k(\theta_d - \alpha) + c\dot{\theta}_d \geq 0, & \forall \dot{\theta}_d \end{cases} \right\}$$

$$A^- = \left\{ (\theta_d, \dot{\theta}_d) : \begin{cases} f(\theta_d - \alpha, \dot{\theta}_d) \leq -2\alpha, & \dot{\theta}_d < 0 \\ k(\theta_d + \alpha) + c\dot{\theta}_d \leq 0, & \forall \dot{\theta}_d \end{cases} \right\}$$

$$A^0 = \{(\theta_d, \dot{\theta}_d)\} \setminus (A^+ \cup A^-)$$

$$f(\theta_d + \alpha, \dot{\theta}_d) \approx (\theta_d + \alpha) + (c\dot{\theta}_d / k) e^{-k(\theta_d + \alpha)/c\dot{\theta}_d - 1} = 2\alpha$$

$$T = \begin{cases} 0 \ \ or \ \ k(\theta_d - \alpha) + c\dot{\theta}_d + j\ddot{\theta}_d & \theta_d + (c/k)\dot{\theta}_d + (j/k)\ddot{\theta}_d > \alpha \\ 0 & \left|\theta_d + (c/k)\dot{\theta}_d + (j/k)\ddot{\theta}_d\right| \leq \alpha \\ 0 \ \ or \ \ k(\theta_d + \alpha) + c\dot{\theta}_d + j\ddot{\theta}_d & \theta_d + (c/k)\dot{\theta}_d + (j/k)\ddot{\theta}_d < -\alpha \end{cases} \quad (5)$$

The fifth equation represents the new approach being analyzed in this paper, and will be compared to the approaches 2 to 4.

2.1 Magnitude of Transmitted Torque

The expression of the torques from Equations (2) to (5) are such that starting from (2) each next expression is an enhancement of the previous. While in Equations (2) to (4) only the damping and elasticity effect are included in the approximation, Equation (5) takes additionally into account the inertia and should be closer to real physical systems [3]. One can see that, either only the intervals are enhanced as in the case from (2) to (4) or the magnitude of the torque is also enhanced as in (5). Considering only the torque expressions (without the backlash boundaries), these logical enhancements lead to the following limiting expressions:

$$\underset{j \to 0}{Limit} \ \ Equation\ (5) = Equations\ (4)\ \&\ (3) \quad (6)$$

$$\underset{c \to 0}{Limit} \ \ Equations (4)\ \&\ (3) = Equation\ (2) \quad (7)$$

$$\underset{(j,c) \to (0,0)}{Limit} \ \ Equation(4) = Equation(2) \quad (8)$$

Thus it can be seen that there is convergence in the models according to the above limiting expressions. The fact that the expression of the transmitted torques are different, leads to the suggestion that, the magnitude of the transmitted torques of equations (2) to (4) are different from (5). This can be demonstrated by setting $\alpha = 0$ in equations (2) to (5). In that case, there is no backlash and the system can be considered as continuous. Observe that only equation (5) reduces to the torque expression of a rotating system approximated as a Single-Degree-of-Freedom (SDOF where $T = k(\theta) + c\dot{\theta} + j\ddot{\theta}$). Thus equation (5) is more likely to approximate the system behavior closer. To show that (5) approximates better than the others, it suffices to choose a single combination of j, c and k for which it predicts real system behavior closer than the others. Using the system properties $j = [10 Kgm^2]$, $c = 5[Nm/rad/s]$ $k = 10[Nm/rad]$ and $\alpha = 0[rad]$ with an arbitrary sinusoidal input the following graphs in Fig 2 (a) depict the behavior of the different models.

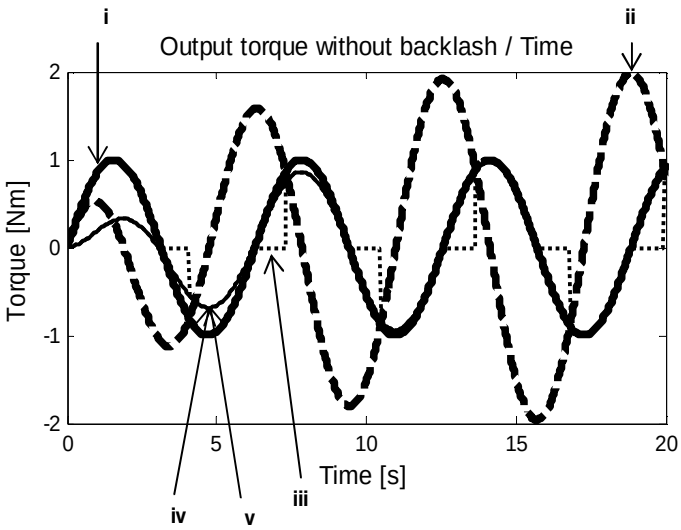

Fig 2 (a) Torque versus time

Where:

i. Input torque
ii. Output torque of the continous shaft
iii. Output torque of phase plane model (Eq 4)
iv. Output torque of physical system used in developing the phase plane model (Eq.3)
v. Modified dead zone model (Eq. 2)

In Fig 2 (a), it can be seen that the curve depicting the behaviour of the continous shaft at resonance is different from all the others in magnitude and phase. It can also be seen that though the phase plane model (iii) has a step, in general the phase and magnitude are similar to those of the iv. And v. due to their convergence. This is contrary to expectation since the backlash was set to zero and should therefore approximate to the continuous system. On the other hand, Fig 2 (b) shows a perfect match between the new model (JCK-model) and the continous shaft.

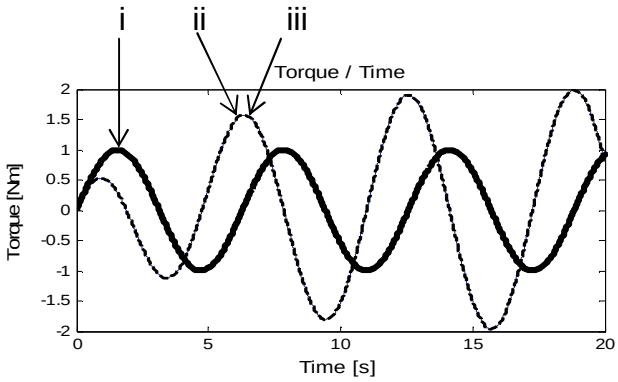

Fig. 2(b) Torque vs time

Where:

i. Input torque
ii. Output torque of continous shaft
iii. Output torque of proposed backlash model (JCK-model)

As was shown earlier, the transmitted torques are given by different expressions. Consequently their curves are different as observed from the graphs above. The JCK model reflects reality more which can be seen from its convergence with the continuous system when its backlash is set to zero.

2.2 Intervals of Transmitted Torque

In order to illustrate further discrepancies, the backlash boundaries expressions of Equations (2), (3) and (5) are examined. Equation (4) is not considered in this section because it is simply a derivative of (3) and also does not consider the inertia. The solutions to the interval expressions are obtained assuming the following initial conditions: at $t = 0$, $\dot{\theta} = \ddot{\theta} = 0$ i.e. the shaft starts from rest. We also assume that the system has a backlash angle such that $\alpha = 1rad$. Let the shaft also be arbitrary with the following properties: $j = 10\left[Kgm^2\right]$, $c = 10\left[Nm/rad/s\right]$ and $k = 5\left[Nm/rad\right]$.

These graphs show the intervals where the torques act, with the X-axis as a symmetric axis as illustrated in Fig. 5 below.

In order to understand the graphs let us consider the plot (Fig. 3) of the backlash boundary expressions from the massless beam used in developing the phase plane model [1, 2] (Equation (3), noted as massless beam for the phase plane model (PPM)). It can be observed that this graph is symmetric relative to the X-axis. The upper half plot represents the right contact above which the torque is non-zero (region A). The lower half plot represents the left contact below which the torque is non-zero (region C). The area between the upper and lower halves is the free play region with a torque of zero (region B).

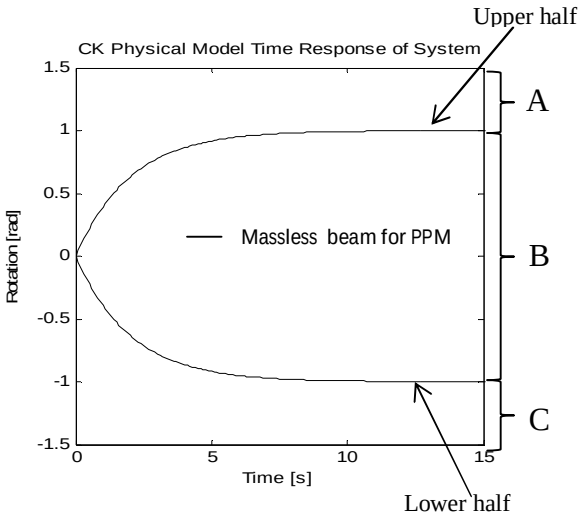

Fig. 3 Interval plot: phase plane model's physical system (Equation 3)

The different regions are governed by the following expressions:

A: $T=0 \quad or \quad k(\theta_d-\alpha)+c\dot{\theta}_d; \quad \theta_d+(c/k)\dot{\theta}_d>\alpha$

B: $T=0; \qquad \left|\theta_d+(c/k)\dot{\theta}_d\right|\le\alpha$

C: $T=0 \quad or \quad k(\theta_d+\alpha)+c\dot{\theta}_d; \quad \theta_d+(c/k)\dot{\theta}_d<-\alpha$

If we now superimpose the discussed plot with the interval plot of the modified dead zone model we get the following (Fig. 4):

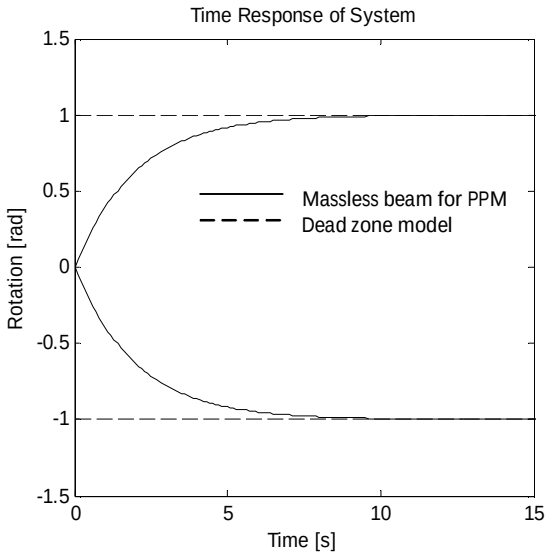

Fig. 4 Superimposed intervals

Observe that both graphs; the modified dead zone model in dash lines and the physical system of the phase plane massless beam model in continuous line converge over time. Introduce mass into the beam with $j=10\left[Kgm^2\right]$, results in additional graph shown Fig. 5 below. It can be observe that though all three modeling approaches converge over time. The massless beam for PPM and the mass beam models predict the physical system behavior better than the modified dead zone model because one can clearly see when the system comes in contact with the boundaries. This is because in addition to the elasticity of the shaft they also take into account the damping effects (first order approximation). On the other hand the mass model goes even further to approximate the system as a second order through the additional consideration of the system's inertia, thus making it even better than its counterpart.

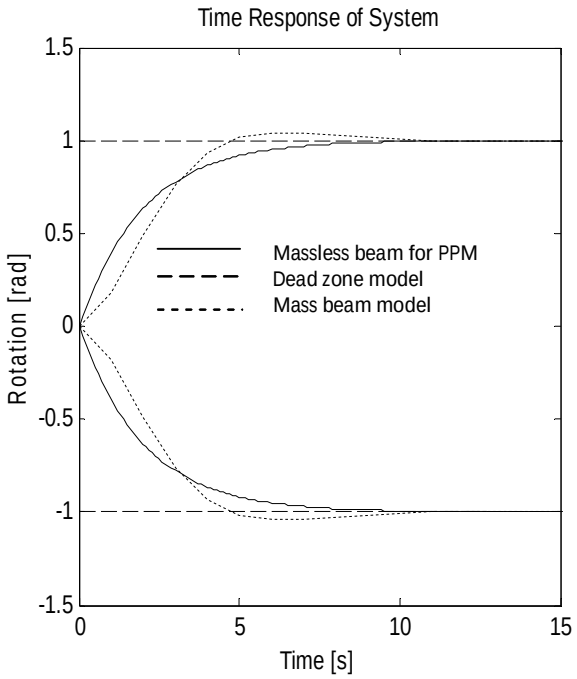

Fig. 5 Superimposed intervals of all three models

Observe that the inertia (mass) model exhibits the systems tendency to resists motion induced by an external moment. A good observation to make here is that, the mass model approaches the boundaries twice as fast (5 seconds) as the massless beam for PPM model (10 seconds). It can also be observed that the curves cross each other which indicate that the behavior of the system within the backlash zones with a positive, zero or negative torque equally vary depending on the approximation of the beam. From theory, Equation (5) actually reflects more the physical behavior of a real system. Since the massless approach does not predict the system behavior exactly, it is therefore worth considering the JCK model for backlash modeling because it takes into account the contribution of the inertia and should lead to more accurate system behavior and sizing.

A further difference can be seen when plotting the rotation velocity regions of the Massless beam for PPM (continuous curve) and the

proposed model (dash curve) as shown in Fig. 6 below:

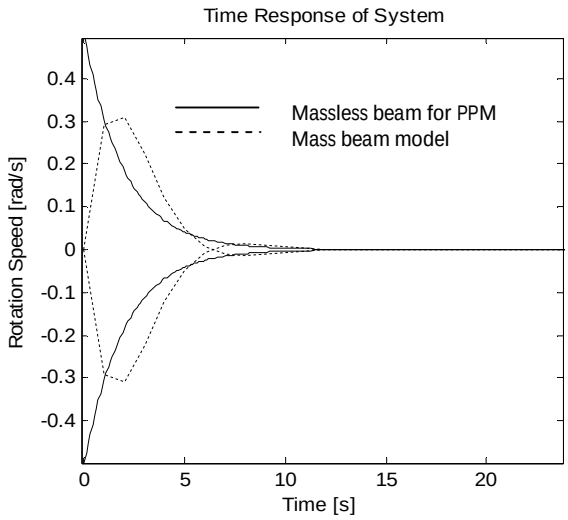

Fig. 6 Superimposed velocity intervals

Fig. 6 shows convergence of the plots over time but a mismatch of the approximations at the beginning, even with a crossing of the curves for the mass model. It can be observed that though the motion of the system starts from rest according to the initial conditions above, the continuous curve does not reflect these conditions, giving a direct observation on the limitation of the massless beam assumption. This difference is as a result of the orders of the differential equations used in modeling the system, where the Mass beam model is a second other approximation unlike the massless beam which is a first order approximation.

3 Failure mode simulation analysis

A simple failure case was simulated and the behavior of the output rotation observed and compared. Here a linear input (i) shown in Fig 8 (a) was used. The failure mode simulated was a pseudo-shaft rupture where the input torque was abruptly set to zero during simulation. The block diagram representation of the Simulink models of Equations (2) to (5) is shown in Fig. 7 below.

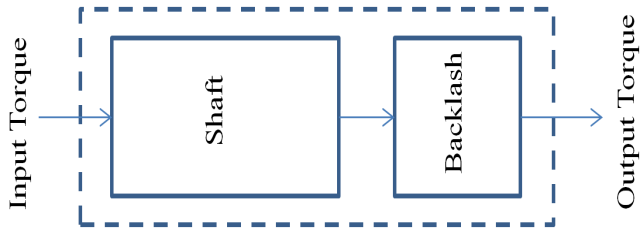

Fig 7 Modeling method

For this simulation, the following system parameters were used: $j = 50[Kgm^2]$; $c = 10[Nm/rad/s]$; $k = 0.01[Nm/rad]$, and a backlash angle such that $\alpha = 0.01\ [rad]$. The backlash zones of the models are shown in Fig. 8 below:

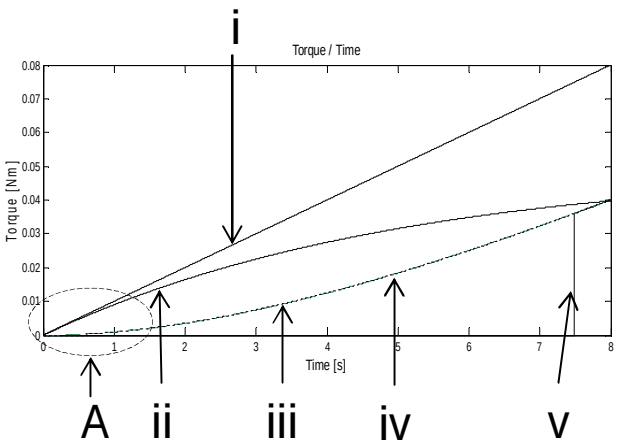

Fig 8 (a) Free-play regions of the different backlash models

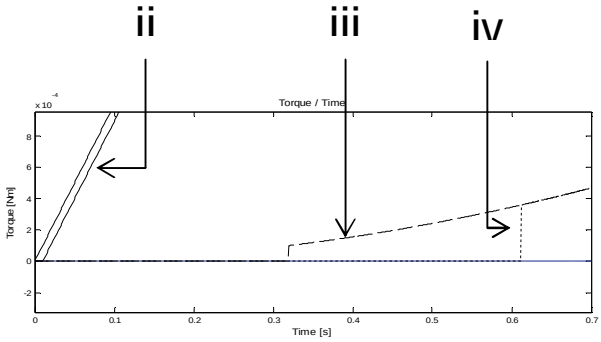

Fig 8 (b) Zoomed plot of Region A

Where the torques are according to Table 1 below:

ID	Torque
i	Input torque
ii	Output torque of proposed model (Eq. 5)
iii	Output torque of physicakl system used in developing the phase plane model (Eq. 3)
iv	Phase plane model (Eq. 4)
v	Modified dead zone model (Eq. 2)

Table 1 Torques and IDs

All models show different response times for which the output torque becomes non-zero. In this case, the response time is considered as the time needed by the system to get out of the backlash zone. This difference is a result of the different approximations of the models which account for different times need for torque to be transmitted from one end of the shaft to the other. The response time of the modified dead zone model is the largest while that of the proposed model is the smallest. After 10 seconds of simulation time the failure was simulated and the various profiles from the different models are plotted in Figure 9 below:

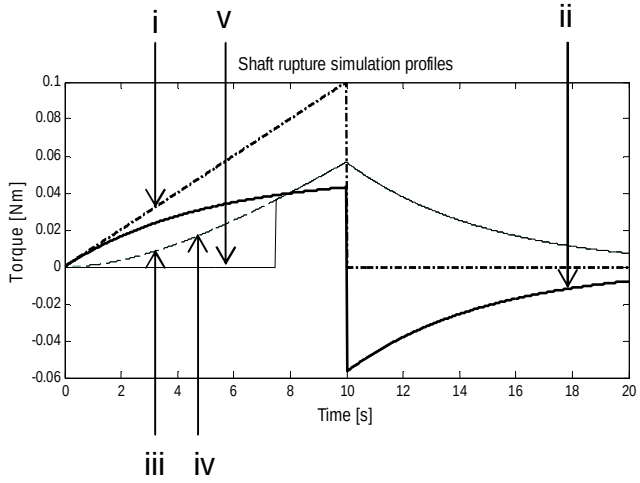

Fig 9 Shaft's rupture failure simulation profiles

Where the torques (i) to (v) are according to table 1 above.

In Fig 9, after around $t = 7s$, a convergence can be seen in all other models (iii, iv, v) except the proposed model (ii). At $t = 10s$ the input torque (i) is abruptly set to zero. While all models except the proposed model have a slope that approaches zero with a negative gradient from the time of rupture, the proposed model shows a sudden flip in the torque as a result of the rupture and further reduces to $T = 0$ with a positive gradient. The behavior of the proposed model is closer to that of an SDOF because of this reversal of torque, which normally occurs in any situation where the action force abruptly goes to zero in a situation of opposing action and reaction forces. A consequence of this unexpected behavior in the old models is that, vibration studies of systems may not be very accurate because if the mass of the system is not considered then the models may portray inaccurate system behavior, different from system with mass as shown in the case in Fig. 9. This may lead to wrong natural frequency calculations, wrong damping values, etc. On the other hand the new model reflects real system behavior better because it captures certain system behaviors not seen in the other models such as the case of shaft rupture in Fig 9 and the resonance behavior of Fig 2.

4 Analytic proof of proposed backlash model (JCK)

To validate this model, an analytic proof of concept is presented at the Appendix (**Section 6**). As a summary in this section, the analytic proof comprise of the approach and theorems taken from [1] and [2] used in the development of the phase plane analysis. From Fig. 1, the torque on the left hand side (T) acts upon a system with the following properties: inertia (j), torsional spring elasticity (k), and internal damping constant (c). T_0 is the output torque. As represented in Fig. 1, let θ_1 be the angle of the input side of the shaft, θ_3 the angle of the driving axis at the backlash, and θ_2 the angle of the driven member. Examining the model shown in Fig. 1, one can easily deduce an exact expression of the torque using Newton's law of motion to obtain its corresponding equation of motion as:

$$T(t) = j\ddot{\theta}_s + c\dot{\theta}_s + k\theta_s = j\left(\ddot{\theta}_d - \ddot{\theta}_b\right) + c\left(\dot{\theta}_d - \dot{\theta}_b\right) + k(\theta_d - \theta_b) \quad (9)$$

Where $\theta_s = \theta_d - \theta_b$ and $\theta_b = \theta_3 - \theta_2$

Here the torque (T) is formulated as a function of angular displacement, velocity and acceleration using of θ_1 and θ_2 without the use of θ_3. It is equally shown that there is contact when system surpasses the backlash zone and no contact within it. For a complete proof please refer to the Appendix, section 6.

5 Conclusion

It was demonstrated that the new model with mass consideration converges to the phase plane model and the massless beam model as the mass of the beam approaches zero. If in addition, the damping of the shaft is reduced to approach zero, then, all three models can be approximated by the modified dead zone model. From the differences observed in the magnitude, regions and failure analysis, physical system behavior can be better approximated using the new model (equation (5)) with mass consideration for estimating the backlash effect in drivetrains. Worthy to note is that the phase plane model was developed using a massless beam, thus inertia is not considered. On the other hand the new model takes into account the mass of the beam; hence it contains extra system behaviors that are not observed in either the phase plane model or the other models mentioned above. The results of this investigation predict new conditions (different from the other models) for determining when there is right or left contact within the backlash region. Using appropriate expressions for the torques, their formulation and validation is shown in the Appendix, section 6. The state space derivative from equation (5) as shown in the appendix, yields the following expression:

$$\ddot{\theta}_b + \frac{c}{j}\dot{\theta}_b = \begin{cases} \max\left(0, \ddot{\theta}_d + \frac{c}{j}\dot{\theta}_d + \frac{k}{j}(\theta_d - \theta_b)\right), & \theta_b = -\alpha \quad (T \le 0) \\ \ddot{\theta}_d + \frac{c}{j}\dot{\theta}_d + \frac{k}{j}(\theta_d - \theta_b), & |\theta_b| < \alpha \quad eq\ 20 \\ \min\left(0, \ddot{\theta}_d + \frac{c}{j}\dot{\theta}_d + \frac{k}{j}(\theta_d - \theta_b)\right), & \theta_b = \alpha \quad (T \ge 0) \end{cases}$$

…(*)

(*) is henceforth presented as a new method in estimating backlash. In combination with (*), equation (9) can be used to determine the transmitted torque.

The advantage of the proposed model is that, one gets not only a better backlash region behavior, but also the right magnitude of transmitted torque. The next step is to validate the approach with measured data.

References

[1] M. Nordin., J. Galic and P. Gutman., "New Models for Backlash and Gear Play", *International Journal of Adaptive Control and Signal Processing*, Vol. 11, 1997, pp. 49-63.

[2] G. Tao., F. L. Lewis. (Eds.): *Adaptive Control of Nonsmooth Dynamic System*, Springer-Verlag London Limited, Great Britain, 2001, Chap. 1.

[3] A. Brandt.: *Introduction to Noise and Vibration Analysis*, Saven EduTech AB, Täby, Sweden, 2001.

[4] A. Lagerberg.: "Control and Estimation of Automotive Powertrains with Backlash," Ph.D. Dissertation, Department of Signals and Systems, Chalmers University of Technolgy, Göteborg, Sweden 2004.

[5] M. Tallfors., "Parameter Estimation and Model Based Control Design of Drive Train Systems," Licentiate Thesis, Kungliga Tekniska Högskolan, Stockholm, Sweden, 2005.

[6] A. Lagerberg., Bo S. Egardt.: "Backlash Gap Positioning Estimation in Automotive Powertrains," European Control Conference, Cambridge, UK, 2003.

[7] J. H. Baek., Y. K. Kwak and S. H. Kim: "Analysis on the influence of Backlash and Motor Input Voltage in Geared Servo System" The 11th Mediterranean Conference on Control and Automation, Rhodes, Greece, 2003.

APPENDIX

6 Complete analytic proof of proposed backlash model (JCK)

To validate this model, a complete analytic proof of concept is presented here. As was stated under section 4 above, the goal is to formulate the torque (T) shown in equation (9) above as a function of angular displacement, velocity and acceleration using of θ_1 and θ_2 without the use of θ_3.

6.1 Assumptions

The following assumptions are made:

- The impact when the backlash gap is closed is inelastic
- Contact can occur between the driving and driven members on either side of the backlash

6.2 Definitions

The following definitions are used:

- **Right contact:** $\theta_b = \alpha$, $\dot{\theta}_b = \ddot{\theta}_b = 0$
- **Left contact:** $\theta_b = -\alpha$, $\dot{\theta}_b = \ddot{\theta}_b = 0$
- **Contact:** ‘Contact’ if there is either left or right contact

T > 0 implies right contact, because otherwise no positive torque could be transmitted. Combining this condition with equation (9) yields:

$$T(t)>0 \Rightarrow T(t)= j\left(\ddot{\theta}_d - 0\right)+c\left(\dot{\theta}_d - 0\right)+k\left(\theta_d - \alpha\right)=\ldots$$

$$j\ddot{\theta}_d + c\dot{\theta}_d + k\left(\theta_d - \alpha\right) > 0 \qquad (10)$$

Similarly, T < 0 implies left contact. This condition in combination with Equation (9) yields:

$$T(t)<0 \Rightarrow T(t)= j\left(\ddot{\theta}_d - 0\right)+c\left(\dot{\theta}_d - 0\right)+k\left(\theta_d + \alpha\right)=\ldots$$

$$j\ddot{\theta}_d + c\dot{\theta}_d + k\left(\theta_d + \alpha\right) < 0 \qquad (11)$$

Logical negation of (10) and (11) yields:

$$\begin{cases} k(\theta_d - \alpha) + c\dot{\theta}_d + j\ddot{\theta}_d & \Rightarrow \quad T \geq 0 \\ k(\theta_d + \alpha) + c\dot{\theta}_d + j\ddot{\theta}_d & \Rightarrow \quad T \leq 0 \end{cases} \qquad (12)$$

Respectively, equations (9) to (12) lead to equation (5). From the expression of the torque in Equation (12) we can define the following areas:

$$A^+ = \left\{\left(\theta_d, \dot{\theta}_d, \ddot{\theta}_d\right): j\ddot{\theta}_d + c\dot{\theta}_d + k\theta_d \geq k\alpha \right. \qquad (13)$$

$$A^r = \left\{\left(\theta_d, \dot{\theta}_d, \ddot{\theta}_d\right): \left| j\ddot{\theta}_d + c\dot{\theta}_d + k\theta_d \right| < k\alpha \right. \qquad (14)$$

$$A^- = \left\{\left(\theta_d, \dot{\theta}_d, \ddot{\theta}_d\right): j\ddot{\theta}_d + c\dot{\theta}_d + k\theta_d \leq -k\alpha \right. \qquad (15)$$

Where A^r represents the interior free play gap of the backlash.

6.3 Lemma 1

During a non-zero interval, persistent right contact is only possible in A^+ and persistent left contact only in A^-.

Proof by contradiction:

a) **Persistent right contact only in A^+:**

We assume right contact outside A^+. From (9) and (13), it follows that:
$T = j\ddot{\theta}_d + c\dot{\theta}_d + k\theta_d - k\alpha < 0$
Hence a persistent negative torque with right contact implies a pull force which is physically impossible. Hence we can only have a persistent right contact in A^+.

a) Persistent left contact only in A^-:

We assume right contact outside A^-. From (9) and (15), it follows that:
$T = j\ddot{\theta}_d + c\dot{\theta}_d + k\theta_d + k\alpha > 0$
Hence a persistent positive torque with left contact implies a push force which is physically

impossible. Hence we can only have a persistent left contact in A^-.

6.4 Lemma 2:

If the system state $(\theta_d, \dot{\theta}_d, \ddot{\theta}_d)$ at the initial time $t = t_0$ lies in A^+ with $\theta_b(t_0) = \alpha$ (right contact), with $\theta_b(t_0) = \alpha$, $\forall t_1 > t_0$: $(\theta_d, \dot{\theta}_d, \ddot{\theta}_d) \in A^+$ for all $t \in [t_0 \quad t_1]$.

If $(\theta_d(t_0), \dot{\theta}_d(t_0), \ddot{\theta}_d(t_0)) \in A^-$ with $\theta_b(t_0) = -\alpha$ (left contact), then $\theta_b(t_1) = -\alpha$ for all times $t_1 = t_0$ such that $(\theta_d(t), \dot{\theta}_d(t), \ddot{\theta}_d(t)) \in [t_0 \quad t]$

a) Proof of right contact:

Right contact in the interior of A^+ together with (9) implies that $T > 0$. Right contact is maintained as long as there is positive torque. At the boundary of A^+, i.e. with $j\ddot{\theta}_d + c\dot{\theta}_d + k\theta_d = k\alpha$, it holds from (5) that $T = 0$ and together with (9) this yields to:

$$T(t) = j(\ddot{\theta}_d - \ddot{\theta}_b) + c(\dot{\theta}_d - \dot{\theta}_b) + k(\theta_d - \theta_b) = 0$$
$$\Rightarrow \quad T = j\ddot{\theta}_d + c\dot{\theta}_d + k\theta_d - (j\ddot{\theta}_b + c\dot{\theta}_b + k\theta_b) = 0$$

But $j\ddot{\theta}_d + c\dot{\theta}_d + k\theta_d = k\alpha$

$$\Rightarrow \quad j\ddot{\theta}_b + c\dot{\theta}_b + k\theta_b = k\alpha \qquad (16)$$

To solve (16) we use the following conditions: Steady state condition: $\theta_b = \alpha$, $\dot{\theta}_b = \ddot{\theta}_b = 0$ and the initial condition with $t = t_0$. With consideration of these conditions,

$$\theta_b(t) = Ae^{\lambda_1 t_0} + Be^{\lambda_2 t} + \alpha \qquad (17)$$

With:

$$A = \frac{\dot{\theta}_b(t_0)}{\lambda_1} e^{-\lambda_1 t_0} - \left[\frac{\lambda_1\theta_b(t_0) - \dot{\theta}_b(t_0) - \lambda_1\alpha}{\lambda_1 - \lambda_2}\right]\frac{\lambda_2}{\lambda_1} e^{-\lambda_1 t_0}$$

and

$$B = \frac{\lambda_1\theta_b(t_0) - \dot{\theta}_b(t_0) - \lambda_1\alpha}{e^{\lambda_2 t_0}(\lambda_1 - \lambda_2)}$$

Starting with right contact ($\theta_b = \alpha$), equation (17) becomes a constant $\theta_b = \alpha$, thus right contact is preserved.

The symmetric proof applied to the left contact and the trajectory in A^- is as follows:

b) Proof of left contact

Left contact in the interior of A^- together with (9) implies that $T < 0$. As long as there is negative torque, left contact is maintained. At the boundary of A^-, i.e. with $j\ddot{\theta}_d + c\dot{\theta}_d + k\theta = -k\alpha$, it holds from equation (5) that $T = 0$ and together with (9) this yields to:

$$T(t) = j(\ddot{\theta}_d - \ddot{\theta}_b) + c(\dot{\theta}_d - \dot{\theta}_s) + k(\theta_d - \theta_b) = 0$$
$$\Rightarrow \quad T = j\ddot{\theta}_d + c\dot{\theta}_d + k\theta_d - (j\ddot{\theta}_b + c\dot{\theta}_b + k\theta_b) = 0$$

But $j\ddot{\theta}_d + c\dot{\theta}_d + k\theta_d = -k\alpha$

$$\Rightarrow \quad j\ddot{\theta}_b + c\dot{\theta}_b + k\theta_b = -k\alpha \qquad (18)$$

To solve (18) we use the following conditions: When $\theta_b = -\alpha$, $\dot{\theta}_b = \ddot{\theta}_b = 0$ (steady state condition) and let the initial time $t = t_0$ (initial condition), then we have that:

$$\theta_b(t) = Ae^{\lambda_1 t_0} + Be^{\lambda_2 t} - \alpha \qquad (19)$$

With:

$$A = \frac{\dot{\theta}_b(t_0)}{\lambda_1} e^{-\lambda_1 t_0} - \left[\frac{\lambda_1\theta_b(t_0) - \dot{\theta}_b(t_0) - \lambda_1\alpha}{\lambda_1 - \lambda_2}\right]\frac{\lambda_2}{\lambda_1} e^{-\lambda_1 t_0}$$

and

$$B = \frac{\lambda_1\theta_b(t_0) - \dot{\theta}_b(t_0) + \lambda_1\alpha}{e^{\lambda_2 t_0}(\lambda_1 - \lambda_2)}$$

Starting with left contact ($\theta_b = -\alpha$), equation (19) becomes a constant $\theta_b = -\alpha$ thus, left contact is preserved.

6.5 Theorem (Release condition):

We assume that $\theta_b(t_0)=\alpha$ or $\theta_b(t_0)=-\alpha$, thus we have contact at time t_0. Contact is lost at the first time $t_1>t_0$ such that the trajectory $(\theta_d,\dot{\theta}_d,\ddot{\theta}_d)$ reaches the release set A^r.

Proof

This follows from the fact that right respectively left contact cannot be lost in A^+ respectively A^-, and that in A^r, which lies between A^+ and A^-, contact is not possible. When contact is lost we know that $T=0$ and equation (9) leads to:

$$\ddot{\theta}_d-\ddot{\theta}_b+\frac{c}{j}\left(\dot{\theta}_d-\dot{\theta}_b\right)+\frac{k}{j}\left(\theta_d-\theta_b\right)=0 \qquad (20)$$

Letting $x=\theta_d-\theta_b$ and solving the above equation, we get:

$$\theta_b(t)-\theta_d(t)=Ae^{\lambda_1 t_0}+Be^{\lambda_2 t} \qquad (21)$$

With:

$$A=\left[\frac{\lambda_1 x(t_0)-\dot{x}(t_0)}{\lambda_1-\lambda_2}\right]\frac{\lambda_2}{\lambda_1}e^{-\lambda_1 t_0}-\frac{\dot{x}(t_0)}{\lambda_1}e^{-\lambda_1 t_0}$$

and $B=\dfrac{\dot{x}(t_0)-\lambda_1 x(t_0)}{e^{\lambda_2 t_0}(\lambda_1-\lambda_2)}$

With: $x(t_0)=\theta_d(t_0)-\theta_b(t_0)$ and $\dot{x}(t_0)=\dot{\theta}_d(t_0)-\dot{\theta}_b(t_0)$

Since θ_d, $\dot{\theta}_d$ and $\ddot{\theta}_d$ are given and equation (21) gives θ_b, equation (22) gives $\dot{\theta}_b$ and $\ddot{\theta}_b$ Furthermore, when $|\theta_b|=\alpha$, contact is achieved. Solving for θ_b as a state space model, an exact solution is obtained.

Using equation (19), $|\theta_b|\le\alpha$ and the release condition we get:

$$\ddot{\theta}_b+\frac{c}{j}\dot{\theta}_b=\begin{cases}\max\left(0,\ddot{\theta}_d+\frac{c}{j}\dot{\theta}_d+\frac{k}{j}(\theta_d-\theta_b)\right), & \theta_b=-\alpha \quad (T\le 0)\\ \ddot{\theta}_d+\frac{c}{j}\dot{\theta}_d+\frac{k}{j}(\theta_d-\theta_b), & |\theta_b|<\alpha \quad eq\ 20\\ \min\left(0,\ddot{\theta}_d+\frac{c}{j}\dot{\theta}_d+\frac{k}{j}(\theta_d-\theta_b)\right), & \theta_b=\alpha \quad (T\ge 0)\end{cases}$$

… (22)

An interpretation of this state equation would be a limited integrator with the time derivative $\ddot{\theta}_d+\frac{c}{j}(\dot{\theta}_d-\dot{\theta}_b)+\frac{k}{j}(\theta_d-\theta_b)$ and limiter α. From equation (22), θ_b, $\dot{\theta}_b$ and $\ddot{\theta}_b$ are known and given θ_d, $\dot{\theta}_d$ and $\ddot{\theta}_d$, the torque T is found by equation (9). The expression above describes a non-linear dynamical system, not a function, that gives the torque T with given θ_d, $\dot{\theta}_d$ and $\ddot{\theta}_d$. The derivation demonstrates that this new formula for modeling backlash incorporates contact and persistent contact depending of the direction of the applied torque at the boundaries of the free play region as well as no contact within the free play region.